

29

Convection

Convection is a major driving agent behind most of the weather phenomena in the atmosphere, from ordinary cyclones to hurricanes and thunderstorms and tornadoes. Continental drift on Earth as well as transport of heat from the center of a planet or star to the surface are also mainly driven by convection. At a smaller scale, we use heat convection in the home to create a natural circulation which transports heat around the rooms from the radiators of the central heating system. Earlier, the circulation of water in the central heating system was also driven by convection, but is today mostly driven by pumps.

The mechanism behind convection rests on a combination of material properties and gravity. Most fluids, even those we call incompressible, tend to expand when the temperature is raised, leading to a slight decrease in density. Were it not for gravity, the minuscule changes in density caused by local temperature variations would be of very little consequence, but gravity makes the warmer and lighter fluid buoyant relative to the colder and heavier, and the buoyancy forces will attempt to set the fluid into motion. Such heat-driven motion is called *convection*, and will in fact arise naturally wherever there are sufficiently large local variations in the temperature of a fluid.

In this chapter we shall first discuss some examples of steady laminar convection flows driven by time independent temperature differences on the container boundaries. Afterwards we shall address the thermal instabilities characterizing the onset of convection. Of particular interest are the Rayleigh-Bénard instabilities in a horizontal layer of fluid heated from below.

29.1 Convection

Convection is caused by buoyancy forces in combination with the tendency for most materials to expand when heated¹. The coupled partial differential equations controlling the interplay of heat and motion are generally so complex that exact solutions are completely out of the question. Numeric simulations are, however, possible and used wherever practical problems have to be solved. Analytic insight into convection is mainly obtained from an approximation developed by Boussinesq in 1902.

Thermal expansion coefficient

The (isobaric) *coefficient of thermal expansion* is for all kinds of isotropic matter defined as the relative decrease in density per unit of temperature raise (at constant pressure),

$$\alpha = -\frac{1}{\rho} \left(\frac{\partial \rho}{\partial T} \right)_p, \quad (29-1)$$

It is a material “constant” which for ideal gases where $\rho \propto p/T$ becomes $\alpha = 1/T$, or about $3 \times 10^{-3} \text{ K}^{-1}$ at room temperature. For most liquids it is also of this magnitude, the exception being water which has $\alpha \approx 2.5 \times 10^{-4} \text{ K}^{-1}$ at 25 °C. Water is in many respects exceptional with a negative expansion coefficient between 0 and 4 °C, and a solid phase (ice) that is lighter than the liquid.

Turning around the above definition we may calculate the change in density,

$$\Delta \rho = -\alpha \Delta T \rho, \quad (29-2)$$

due to a small change in temperature satisfying $|\alpha \Delta T| \ll 1$. In a constant field of gravity \mathbf{g}_0 , this density change causes an extra gravitational force density $\Delta \rho \mathbf{g}_0$ to appear on the right hand side of the Navier-Stokes equation.

In a flow with velocity scale U , length scale L , and temperature scale Θ , the dimensionless ratio of the buoyancy term to the advective term becomes,

$$\text{Ri} = \frac{|\Delta \rho \mathbf{g}_0|}{|\rho(\mathbf{v} \cdot \nabla) \mathbf{v}|} \approx \alpha \Theta \frac{g_0 L}{U^2}. \quad (29-3)$$

It is called the *Richardson number*, and when this number is small, advection will dominate over convection. Conversely, when it becomes of order unity the flow will be driven by convection with a typical speed $U \sim \sqrt{\alpha \Theta} \sqrt{g_0 L}$, which is the product of the small quantity $\sqrt{\alpha \Theta} \ll 1$ and the free-fall velocity $\sqrt{g_0 L}$ from height $L/2$.

¹Concentration gradients in mixed fluids can also cause convective flow. In this book we reserve the word “convection” to denote a flow that is mainly driven by temperature or concentration differences in conjunction with buoyancy, whereas “advection” is used to denote heat transport in a flow mainly driven by other forces. In practice both mechanisms are at play, and sometimes it is useful instead to distinguish between *free* and *forced* convection.

Lewis Fry Richardson (1881-1953). *British physicist. Applied as the first the method of finite differences to predict weather.*

The Boussinesq approximation

Suppose an effectively incompressible fluid initially is at rest in constant gravity $\mathbf{g}_0 = (0, 0, -g_0)$ with constant density ρ_0 , temperature T_0 , and hydrostatic pressure $p = p_0 - \rho_0 g_0 z$. At a certain time the boundary temperatures are changed, and the resulting flow of heat changes the temperature in the fluid and thereby its density, resulting in turn in a convective flow with velocity field \mathbf{v} .

The main assumption behind the Boussinesq approximation is that the temperature variations are small on the scale set by the thermal expansion coefficient, *i.e.* $|\alpha \Delta T| \ll 1$ where $\Delta T = T - T_0$, and the change in density is to first order given by (29-2) with $\rho = \rho_0$. Adding the buoyancy term $\Delta \rho \mathbf{g}_0 = -\rho_0 \alpha \Delta T \mathbf{g}_0$ to the Navier-Stokes equations, and cancelling off the normal hydrostatic pressure by writing $p = p_0 - \rho_0 g_0 z + \Delta p$, the Boussinesq equations for an effectively incompressible fluid become,

$$\frac{\partial \Delta T}{\partial t} + (\mathbf{v} \cdot \nabla) \Delta T = \kappa \nabla^2 \Delta T, \quad (29-4a)$$

$$\frac{\partial \mathbf{v}}{\partial t} + (\mathbf{v} \cdot \nabla) \mathbf{v} = -\frac{\nabla \Delta p}{\rho_0} + \nu \nabla^2 \mathbf{v} - \alpha \Delta T \mathbf{g}_0, \quad (29-4b)$$

$$\nabla \cdot \mathbf{v} = 0. \quad (29-4c)$$

The complete and correct derivation of the Boussinesq approximation is however not without subtlety (see for example [65, p. 188]).

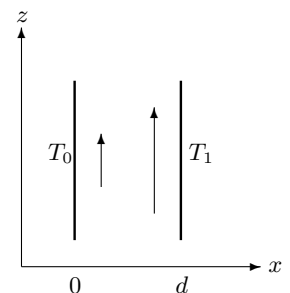
Steady convection in open vertical slot heated on one side

We have previously (page 584) discussed the steady heat flow in a fluid at rest between two plates, one of which was situated at $x = 0$ with temperature T_0 and the other at $x = d$ with higher temperature $T_1 = T_0 + \Theta$. The result was that the temperature rises linearly across the slot. If the plates are vertical, buoyancy forces will act on the heated fluid and unavoidably set it into motion. For definiteness, the plates are assumed to be large but finite with the openings at the top and bottom connected to a reservoir of the same fluid at the same temperature T_0 as the cold plate. This provides the correct hydrostatic pressure at the top and bottom of the slot, a pressure which is necessary to prevent the fluid in the slot from “falling out” under its own weight, even before it is heated. Heating will cause the fluid in the slot to rise and merge with the fluid in the reservoir, and it seems reasonable to expect that a steady flow of heat and fluid may come about, in which the fluid rises fastest near the warm plate. The reservoir is assumed to be so large that it never changes its temperature, except near the exit from the slot.

From the planar symmetry of the configuration we expect that the velocity field is everywhere vertical, and that it and the temperature field depend only on x ,

$$\mathbf{v} = (0, 0, v_z(x)), \quad T = T(x). \quad (29-5)$$

Valentin Joseph Boussinesq (1842-1929). *French physicist and mathematician. Contributed to many aspects of hydrodynamics: whirlpools, solitary waves, drag, advective cooling, and turbulence.*



Steady convection between vertical parallel plates held at different temperatures. The plates continue far above and below the section shown here.

Under these assumptions, there will be no advective contribution to the heat equation (29-4a), which becomes $\nabla_x^2 \Delta T = 0$. The temperature thus varies linearly with x across the slot, and using the boundary conditions we get,

$$\Delta T = \Theta \frac{x}{d}, \quad (29-6)$$

just as in the static case (28-19).

From the assumed form of the velocity field it also follows that the advective term in (29-4b) side vanishes, and from the x, y -components of this equation we conclude that $\nabla_x \Delta p = \nabla_y \Delta p = 0$, so that the pressure can only depend on z . From the z -component we then get

$$\frac{1}{\rho_0} \nabla_z \Delta p(z) = \nu \nabla_x^2 v_z(x) + \alpha \Theta \frac{x}{d} g_0.$$

Since the left hand side depends only on z and the right hand side only on x , both sides of this equation are constant, and since the pressure excess Δp must vanish at the top and bottom of the slot, it must vanish everywhere, $\Delta p = 0$. Using the no-slip boundary conditions on the plates the solution becomes,

$$v_z = \frac{\alpha \Theta g_0 d^2}{6\nu} \frac{x}{d} \left(1 - \frac{x^2}{d^2} \right). \quad (29-7)$$

Notice that the steady flow pattern is independent of the heat diffusivity κ as it would be in forced convection.

The maximal velocity in the slot is found at bit to the right of the middle, at $x = d/\sqrt{3}$. The average velocity in the slot becomes

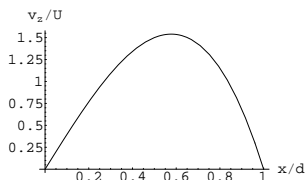
$$U = \frac{1}{d} \int_0^d v_z(x) dx = \frac{\alpha \Theta g_0 d^2}{24\nu}. \quad (29-8)$$

Due to the spurious absence of advection the velocity field scale is set by viscosity rather than by advection. It disagrees with our earlier estimate $\sqrt{\alpha \Theta g_0 L}$ and is a factor $\frac{1}{2} \alpha \Theta$ smaller than the average steady fall velocity through the slot, calculated from (19-10) by setting $G = \rho_0 g_0$. The Reynolds number corresponding to this velocity is

$$\text{Re} = \frac{Ud}{\nu} = \frac{1}{24} \cdot \frac{\alpha \Theta g_0 d^3}{\nu^2}. \quad (29-9)$$

The second factor on the right is called the *Grashof number* and denoted Gr . Formally, the Richardson number becomes $\text{Ri} = 24/\text{Re}$.

Example 29.1.1: For water with $d \approx 1$ cm, $\Theta \approx 10$ K we find $U \approx 12$ cm/s. The corresponding Reynolds number is $\text{Re} \approx 1400$, indicating that the flow should be laminar, as was assumed implicitly in the above calculation. For air the velocity is $U \approx 8$ cm/s and the Reynolds number $\text{Re} \approx 50$.



Convective velocity profile in units of the width of the slot and the average velocity. Its shape is reminiscent of the Poiseuille flow (19-8) although skewed a bit towards the right.

Franz Grashof (1826-93). German engineer who sought to transform machine building into a proper science.

Entrance length for heat

The rate at which heat is transported by convection from the slot into the reservoir may be calculated from the extra internal energy carried by the fluid as it exits the slot,

$$\dot{Q} = \int_0^d \rho_0 c_p \Delta T v_z L dx = \frac{\rho_0 c_p \alpha \Theta^2 g_0 d^3 L}{45 \nu}, \quad (29-10)$$

where L is the size of the slot in the y -direction. This raises a puzzle because the temperature gradient is constant, $\nabla_x \Delta T = \Theta/d$, across the slot, and Fourier's law (28-12) then implies that the same amount of heat is added to the fluid at the warm plate as is removed at the cold. Consequently, no net heat is added to the fluid from the plates, in blatant contradiction with the above calculation and common experience.

What is wrong is the assumption that the solution (29-6) and (29-7) is valid at the bottom of the slot where the fluid enters. Here the temperature gradient cannot be constant, because mass conservation in the steady state forces the cold fluid to enter with the same average velocity U given by (29-8). Since it takes a certain amount of time, $t \approx d^2/4\kappa$, for the heat supplied by the warm plate to diffuse across the slot (see eq. (28-17)), the fluid will have moved through a vertical distance

$$\ell \approx Ut = \frac{\alpha \Theta g_0 d^4}{96 \kappa \nu}, \quad (29-11)$$

before the heat gets into contact with the cold plate. For consistency we should compare the heat loss at the exit (29-10) with the total rate of heat transferred into the fluid in the entrance region. It may be estimated from Fourier's law (28-12) applied to the entrance area $L\ell$. In this region the heated fluid only extends about halfway across the slot leading to a heat flow estimate $\dot{Q} \sim \ell L \cdot k \Theta/(d/2)$, and this is indeed of the same size as the heat loss (29-10) at the exit.

The entrance length may also be written,

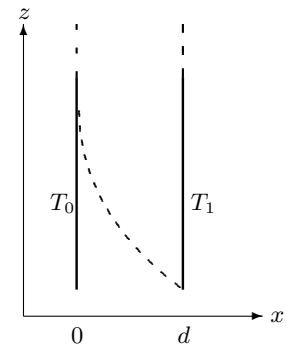
$$\ell \approx \frac{\text{Ra}}{96} d, \quad (29-12)$$

where the dimensionless quantity,

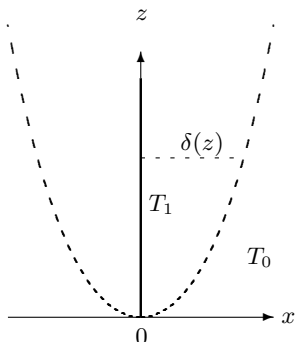
$$\text{Ra} = \frac{\alpha \Theta g_0 d^3}{\nu \kappa}, \quad (29-13)$$

is the famous *Rayleigh number*. In units of the slot width the entrance length for heat ℓ/d is about 1% of the Rayleigh number whereas the viscous entrance length (21-22) in units of the slot width is estimated to be about 2% of the Reynolds number.

Example 29.1.2: In the preceding example 29.1.1 the Rayleigh number for water becomes $\text{Ra} = 2 \times 10^5$, and we get an enormous entrance length $\ell \approx 20$ m, whereas for air we find $\text{Ra} \approx 900$ and a much more manageable $\ell \approx 9$ cm. For comparison the viscous entrance length is 42 cm in water and 1.5 cm in air.



The heat front (dashed) at the entrance to the vertical slot. The heat transferred to the fluid at the warm plate must diffuse across the slot but is at the same time advected upwards with average velocity U . It makes contact with the cold plate after having moved a distance ℓ , called the entrance length for heat.



Outline of thermal boundary layers forming on both sides of a thin plate with constant temperature $T_1 = T_0 + \Theta$, placed vertically in an infinite sea of fluid originally at rest with temperature T_0 . The layer has a z -dependent thickness $\delta(z)$.

* Thermal boundary layer

If the entrance length is much greater than the height of the slot, $\ell \gg h$, the heated fluid will never reach the cold plate before it exits from the slot. In this limit, the cold plate can be ignored, and the appropriate model is instead that of a warm vertical plate with constant temperature placed in a sea of cold fluid. The heated fluid rising along the plate then forms a *thermal boundary layer*, and we shall now determine the steady laminar flow pattern in such a boundary layer by combining the Boussinesq approximation with Prandtl's boundary layer approximation (section 25.3 on page 491).

The coordinate system is chosen with the positive z -axis along the plate. Replacing ℓ by z and d by $\delta(z)$ in the estimate of the heat entrance length (29-11) we obtain an estimate of the z -dependent thickness of the boundary layer (apart from a dimensionless numerical factor),

$$\delta(z) \sim \left(\frac{\kappa \nu z}{\alpha \Theta g_0} \right)^{1/4}. \quad (29-14)$$

Since for $z \rightarrow \infty$ we have $\delta/z \propto z^{-3/4}$ the boundary layer may indeed be viewed as thin, except for a region near the leading edge of the plate.

Under these circumstances we may apply the Prandtl formalism to the Boussinesq equations (29-4) and discard the double derivative after z in the Laplace operators together with the pressure excess Δp . These simplifications lead to the following (Boussinesq-Prandtl) equations for the velocity field, $\mathbf{v} = (v_x, 0, v_z)$, and the temperature excess, $\Delta T = T - T_0$,

$$(v_x \nabla_x + v_z \nabla_z) \Delta T = \kappa \nabla_x^2 \Delta T, \quad (29-15a)$$

$$(v_x \nabla_x + v_z \nabla_z) v_z = \nu \nabla_x^2 v_z + \alpha \Delta T g_0, \quad (29-15b)$$

$$\nabla_x v_x + \nabla_z v_z = 0. \quad (29-15c)$$

These equations must be solved with the boundary conditions that $\Delta T = \Theta$ and $v_x = v_z = 0$ for $x = 0$, and $\Delta T, v_z \rightarrow 0$ for $x \rightarrow \infty$.

Since there is no other possible length scale for x than $\delta(z)$ we shall assume that the fields only depend on x through the variable $x/\delta(z)$, or

$$s = \left(\frac{\alpha \Theta g_0}{\kappa \nu z} \right)^{1/4} x. \quad (29-16)$$

Apart from dimensional prefactors, the fields are parameterized with dimensionless functions of this dimensionless variable,

$$\Delta T = \Theta F(s), \quad v_z = \sqrt{\alpha \Theta g_0 z} G(s), \quad v_x = \left(\frac{\alpha \Theta \kappa \nu g_0}{z} \right)^{1/4} H(s), \quad (29-17)$$

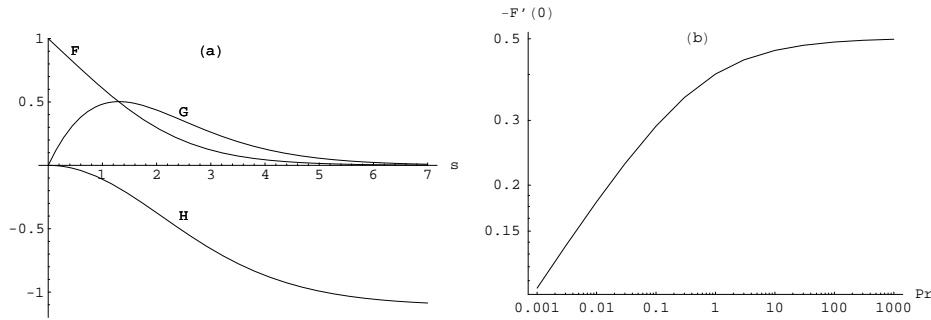


Figure 29.1: Structure of the self-similar thermal boundary layer for $Pr = 1$. (a) Plot of the functions $F(s)$, $G(s)$, and $H(s)$. Notice that asymptotically for $s \rightarrow \infty$ there is a horizontal flow towards the plate which feeds the convective upflow. (b) Doubly logarithmic plot of the heat slope at the plate, $-F'(0)$, as a function of the Prandtl number.

and the field equations become coupled differential equations in s alone,

$$\frac{4}{\sqrt{Pr}}F'' + (sG - 4H)F' = 0, \quad (29-18)$$

$$4\sqrt{Pr}G'' + (sG - 4H)G' + 4F - 2G^2 = 0, \quad (29-19)$$

$$4H' + 2G - sG' = 0, \quad (29-20)$$

where $Pr = \nu/\kappa$ is the Prandtl number. These equations can be solved numerically with the boundary conditions $F(0) = 1$, $G(0) = H(0) = 0$, and $F(\infty) = G(\infty) = 0$. The result is shown in fig. 29.1a for $Pr = 1$. Interestingly, the solution has an asymptotic horizontal flow towards the plate (represented by $H(\infty) = -1.10941\dots$ for $Pr = 1$), rather than a vertical upflow from below, as might have been expected. The divergence of the horizontal velocity for $z \rightarrow 0$ is a spurious consequence of the Prandtl approximation.

The rate of heat flow out of one side of a plate of dimensions $L \times h$ is obtained from Fourier's Law (28-12),

$$\dot{Q} = - \int_{L \times h} k \frac{\partial \Delta T}{\partial x} \Big|_{x=0} dydz = -\frac{4}{3}F'(0) \left(\frac{\alpha \Theta g_0 h^3}{\kappa \nu} \right)^{1/4} k \Theta L. \quad (29-21)$$

The slope $-F'(0)$ is shown in fig. 29.1b as a function of the Prandtl number. The quantity in parenthesis is the Rayleigh number for the height of the plate. Notice that the heat loss, $\dot{Q} \sim \Theta^{5/4}$, grows a little faster than linear.

Example 29.1.3 (Heat radiator): A heat radiator consisting of a single plate of height $h = 70$ cm and width $L = 1$ m is kept at $T = 65$ °C and placed in a room at $T_0 = 20$ °C. For air we have $Pr = 0.73$ and $F'(0) = -0.388$ leading to a total heat flow $\dot{Q} = 235$ W from the radiator (including both sides). The maximal vertical velocity $U = \max v_z$ is quite naturally found at the top of the radiator, $z = h$,

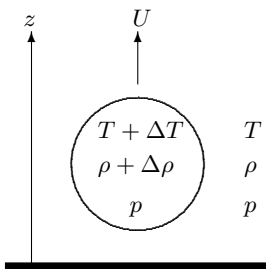
and inspection of fig. 29.1a yields $U = \max_x v_z(x, h) \approx 0.5\sqrt{\alpha\Theta g_0 h} \approx 50 \text{ cm/s}$ at $s = 1.5$ corresponding to a boundary layer width $\delta \approx 1 \text{ cm}$. The horizontal Reynolds number becomes $\text{Re}_\delta = U\delta/\nu \approx 340$, so there should be no turbulence in this boundary layer. The asymptotic horizontal inflow is merely $v_x|_{x \rightarrow \infty} \approx -1 \text{ cm/s}$ at $z = 5 \text{ cm}$ above the bottom of the radiator.

Example 29.1.4 (Human heat loss): For a naked grown-up human the skin surface area is $A \approx 2 \text{ m}^2$, and standing up the height about $h \approx 2 \text{ m}$ and $L \approx 1 \text{ m}$. Taking $\Theta = 10 \text{ K}$ we find the heat loss $\dot{Q} \approx 40 \text{ W}$. Since this is less than half the heat production of 100 W , a human being should easily be able to maintain a skin temperature of 27°C in calm air at 17°C , perhaps by sweating a little (see example 28.2.5). As soon as there is even a very gentle wind, the heat loss grows and rapidly begins to chill the body (see example 28.4.2).

29.2 Convective instability

Fluids with horizontal temperature variations, such as the vertical slot discussed above, cannot remain in hydrostatic equilibrium but must immediately start to convect (see problem 29.9). There is on the other hand nothing in the way of hydrostatic equilibrium if the fluid is only subject to vertical temperature variations $T = T(z)$. If the vertical temperature gradient is positive ($dT/dz > 0$), so that the temperature rises with height, hydrostatic equilibrium is stable because a blob of fluid that is quickly displaced upwards will have lower temperature and higher density than its new surroundings, and thus experience a downwards buoyancy force, tending to bring it down again. Hydrostatic equilibrium may, however, not be stable if the temperature gradient is negative ($dT/dz < 0$) because a blob that is suddenly displaced upwards into a region of lower temperature will experience an upwards buoyancy force which tends to drive it further upwards.

Were it not for drag and heat loss, the displaced blob would rise with ever-increasing velocity. Drag from the surrounding fluid grows with the upwards blob velocity, to begin with linearly. Conductive heat loss lowers the excess temperature of the blob and thereby its buoyancy. Both of these effects grow proportionally with the surface area of the blob whereas buoyancy grows proportionally with the volume, implying that large blobs of fluid tend to be more unstable and rise faster than small. As we shall now see there is a critical blob size below which blobs are not capable of rising at all. In the following section we shall calculate the critical point for onset of instability in particular geometries.



A spherical blob of fluid moving upwards with constant velocity U . If the temperature gradient is negative ($dT/dz < 0$) the temperature of the moving blob will be larger than its surroundings ($\Delta T > 0$). The pressure is assumed to be the same inside and outside the blob.

Stability estimate for spherical blob of fluid

For simplicity we begin with an incompressible fluid at rest in constant gravity g_0 with a constant negative vertical temperature gradient, $dT/dz = -G$, so that the temperature field is of the form $T(z) = T_0 - Gz$. A constant gradient could, as we have seen, be created in a horizontal slot with a fixed temperature difference between the lower and upper plates.

Imagine now that a spherical blob of fluid with radius a is set into upwards motion with an infinitesimally small steady velocity $U > 0$. This is of course a thought experiment, and we do not speculate on the technological difficulties in creating and maintaining such a blob. While it slowly rises towards lower and lower temperatures, the warmer blob will transfer its excess of heat to the colder environment over a typical diffusion time $t \sim a^2/4\kappa$ (see eq. (28-17)). In this time the blob rises through the height $\Delta z \approx Ut \sim Ua^2/4\kappa$, and the environment cools by $\Delta T \sim G\Delta z \sim GUa^2/4\kappa$. In the steady state the competition between the falling temperature of the environment and the loss of heat from the blob should lead to a time independent temperature excess of size ΔT , which in turn determines the buoyancy force.

Unfortunately the estimate of ΔT is a bit weak because the Péclet number $\text{Pe} = 2aU/\kappa$ vanishes in the limit of vanishing U . This implies that for sufficiently small U advection of heat will be negligible compared to diffusion, and that the heat escaping from the blob will spread far beyond the blob radius and thereby raise the temperature of the environment. The rising sphere thus finds itself surrounded by a large “cocoon” of fluid (of its own making) that is warmer than the environment and therefore provides smaller buoyancy than would be the case if the temperature of the environment reigned all the way to the surface of the sphere. So to calculate the buoyancy force we must know the temperature distribution inside the blob relative to the temperature at its surface.

It is most convenient to go to the rest frame of the blob where the flow outside the blob is steady with the temperature of the environment dropping at a constant rate. The true temperature field inside the blob must then be of the form,

$$T' = T_0 - G(z + Ut) + \Delta T, \quad (29-22)$$

where by assumption the temperature excess field ΔT is time independent. Inside the blob, T' must obey Fourier’s heat equation for at fluid at rest (28-14), which under the given assumptions becomes

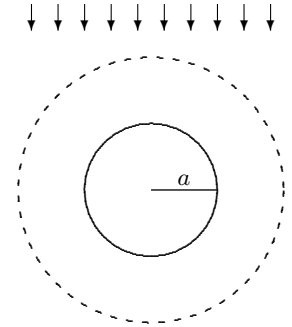
$$-GU = \kappa \nabla^2 \Delta T. \quad (29-23)$$

Seeking a spherical solution, we find $\Delta T = -(GU/6\kappa)r^2 + \text{const}$, and the difference between the temperature inside the blob and on its surface becomes

$$\delta T = \Delta T - \Delta T|_{r=a} = \frac{GU}{6\kappa}(a^2 - r^2). \quad (29-24)$$

This is indeed of the same order of magnitude as the previous estimate $\Delta T \sim GUa^2/\kappa$. The total upwards buoyancy force is obtained from the density change $\delta\rho = -\alpha\delta T\rho_0$ inside the blob,

$$\mathcal{F}_B = \int_V \delta\rho(-g_0)dV = \rho_0 g_0 \alpha \int_0^a \delta T(r) 4\pi r^2 dr = \frac{4\pi\rho_0 g_0 \alpha G a^5 U}{45\kappa}. \quad (29-25)$$



The heat front reaches far beyond the blob radius when the blob velocity is tiny. Here the blob is viewed in its rest frame, where there asymptotically is a uniform downwards wind $-U$ carrying a continually lower temperature.

Evidently, the buoyancy grows like the fifth power of the radius because its volume grows like the third power and the diffusion time like the second.

The viscous drag on a sphere in slow steady motion is given by Stokes Law (20-9),

$$\mathcal{F}_D = 6\pi\eta aU . \quad (29-26)$$

It is valid for small Reynolds number $\text{Re} = 2aU/\nu \ll 1$, a condition which is always fulfilled in the limit of vanishing U .

If the buoyancy is smaller than the drag, $\mathcal{F}_B < \mathcal{F}_D$, the sphere cannot continue to rise on its own. In dimensionless form, this becomes

$$\boxed{\frac{\mathcal{F}_B}{\mathcal{F}_D} = \frac{2}{135} \frac{g_0 \alpha G a^4}{\kappa \nu} < 1 ,} \quad (29-27)$$

where $\nu = \eta/\rho_0$ is the kinematic viscosity (momentum diffusivity) of the fluid. Evidently, this puts an upper limit on the size of stable blobs.

The critical Rayleigh number

In terms of the blob diameter $d = 2a$, the stability condition (29-27) may be written as a condition on the Rayleigh number,

$$\text{Ra} \equiv \frac{g_0 \alpha G d^4}{\kappa \nu} < 1080 . \quad (29-28)$$

Tracing back over the preceding calculation, we see that the large critical value $\text{Ra}_c = 1080$ on the right hand side is mainly due to the ‘‘cocoon’’ of warm fluid carried along with the blob and diminishing its buoyancy. The critical Rayleigh number for blobs of general globular shape may presumably always be taken to be around 1000, whereas blobs with radically different shapes, for example long cylinders, will have quite different critical Rayleigh numbers, although typically they will be large.

Example 29.2.1: For water in a pot on a warm plate held at 50°C in a room with temperature 20°C we have $\Theta \approx 30 \text{ K}$ and a depth of perhaps $h = 10 \text{ cm}$, so that $G = \Theta/h = 300 \text{ K/m}$. The stability limit for spherical blobs is $d \lesssim 3.7 \text{ mm}$, and we expect convective currents to arise spontaneously everywhere in the pot. If instead there is heavy porridge in the pot with heat properties like water but kinematic viscosity, say $\nu \approx 1 \text{ m}^2/\text{s}$, the critical diameter becomes $d \approx 12 \text{ cm}$. Such blobs cannot find room in the container, and only little convection is expected.

If the geometry of a fluid container cannot accommodate blobs larger than a certain diameter d , and if the Rayleigh number for this diameter is below the critical value, the fluid in the container will be stable with the given negative temperature gradient. The critical Rayleigh number depends, however, strongly on the geometry of the container, and cannot in general be calculated analytically. In the following section we shall determine it for the simplest of all geometries, the horizontal slot.

Estimate of terminal blob speed

If the Rayleigh number for a blob is larger than the critical value, $Ra > Ra_c$, the blob will on its own accelerate upwards with larger and larger speed. For large Reynolds numbers form drag on a sphere, $\mathcal{F}_D \approx \frac{1}{4}\rho_0\pi a^2 U^2$ (see page 386), grows quadratically with velocity, and will eventually balance the buoyancy force \mathcal{F}_B . The terminal speed determined by solving $\mathcal{F}_D = \mathcal{F}_B$ becomes for $Ra \gg Ra_c$,

$$U \approx \frac{2}{45} \frac{g_0 \alpha G d^3}{\kappa}, \quad (29-29)$$

where d is the blob diameter. Rising blobs are of course strongly influenced by high speeds, so this is only a coarse estimate.

Example 29.2.2: In example 29.2.1 a water blob with $d = 1$ cm will reach a terminal speed of $U \approx 23$ cm/s, in reasonable agreement with daily experience.

* 29.3 Linear stability analysis of convection

The onset of instability in dynamical systems is usually determined by linearizing the dynamical equations around a particular “baseline” state that may or may not be unstable. The solutions to the linearized dynamics represent the possible fluctuations around the baseline state, and if no fluctuation can grow indefinitely with time, the baseline state will be stable. The existence of a single run-away mode indicates on the other hand that the baseline state is unstable. In the space of parameters that control the system, the condition that all fluctuations be damped leads to an inequality like (29-28), which in the limit of equality defines a *critical surface*, separating the stable region in parameter space from the unstable.

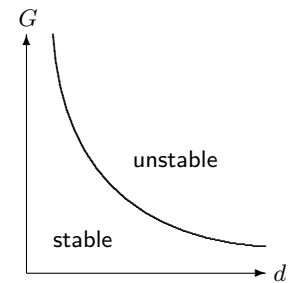
Linearized dynamics of flow and heat

In the present case the baseline state is an incompressible fluid at rest in hydrodynamic equilibrium with a vertical temperature distribution of constant negative gradient, $T = T_0 - Gz$. The pressure must obey the equations of hydrodynamic equilibrium (4-20) on page 65 with the modified density $\rho = \rho_0(1 - \alpha(T - T_0))$ of the heated fluid. Solving the hydrostatic equilibrium equations we find $p = p_0 - \rho_0 g_0 z - \frac{1}{2} \rho_0 g_0 \alpha G z^2$.

A small velocity perturbation \mathbf{v} will generate small corrections to the fields, ΔT and Δp , so that the true temperature and pressure fields become,

$$T = T_0 - Gz + \Delta T, \quad p = p_0 - \rho_0 g_0 z - \frac{1}{2} \rho_0 g_0 \alpha G z^2 + \Delta p. \quad (29-30)$$

To first order in the small quantities ΔT , Δp , and \mathbf{v} , the heat equation (28-23)



Stability plot for heat convection in a system with negative temperature gradient G and size d . The critical surface is $G \sim d^{-4}$.

becomes,

$$\boxed{\frac{\partial \Delta T}{\partial t} - Gv_z = \kappa \nabla^2 \Delta T .} \quad (29-31)$$

Dissipation does not contribute because it is of second order in \mathbf{v} . Adding the buoyancy term $-\alpha \Delta T \mathbf{g}_0 = \alpha \Delta T g_0 \mathbf{e}_z$ to the incompressible Navier-Stokes equation (18-16) we obtain to first order in the small quantities,

$$\boxed{\frac{\partial \mathbf{v}}{\partial t} = -\frac{\nabla \Delta p}{\rho_0} + \nu \nabla^2 \mathbf{v} + \alpha \Delta T g_0 \mathbf{e}_z .} \quad (29-32)$$

The inertial acceleration is absent because it is of second order in \mathbf{v} . Finally the velocity field must satisfy the divergence condition,

$$\boxed{\nabla \cdot \mathbf{v} = 0 .} \quad (29-33)$$

These five coupled partial linear differential equations should now be solved for the five fluctuation fields, ΔT , Δp and \mathbf{v} , with the appropriate boundary conditions for the particular geometry under study.

Fourier transformation

Fourier transformation is method of choice for solving homogeneous linear partial differential equations with constant coefficients. All fields are assumed to be superpositions of elementary harmonic waves of the form $\exp(\lambda t + i\mathbf{k} \cdot \mathbf{x})$ where \mathbf{k} is a real wave vector and λ may be a complex number. For a single harmonic wave, we get from the linearized dynamics,

$$\lambda \Delta \tilde{T} - G \tilde{v}_z = -\kappa \mathbf{k}^2 \Delta \tilde{T} , \quad (29-34a)$$

$$\lambda \tilde{\mathbf{v}} = -\frac{i\mathbf{k}}{\rho_0} \Delta \tilde{p} - \nu \mathbf{k}^2 \tilde{\mathbf{v}} + \alpha \Delta \tilde{T} g_0 \mathbf{e}_z , \quad (29-34b)$$

$$\mathbf{k} \cdot \tilde{\mathbf{v}} = 0 . \quad (29-34c)$$

where now $\Delta \tilde{T}$, $\Delta \tilde{p}$, and $\tilde{\mathbf{v}}$ denote the amplitudes of the harmonic waves. Solving the first equation for \tilde{v}_z , and dotting the second equation with \mathbf{k} (using the third) and solving for $\Delta \tilde{p}$, we obtain,

$$\tilde{v}_z = \frac{\lambda + \kappa \mathbf{k}^2}{G} \Delta \tilde{T} , \quad \frac{\Delta \tilde{p}}{\rho_0} = -\alpha \Delta \tilde{T} g_0 \frac{ik_z}{\mathbf{k}^2} .$$

Inserting this into the z -component of the second equation, we find a linear equation for $\Delta \tilde{T}$, which only has a non-trivial solution for

$$(\lambda + \nu \mathbf{k}^2)(\lambda + \kappa \mathbf{k}^2) = \alpha G g_0 \left(1 - \frac{k_z^2}{\mathbf{k}^2} \right) . \quad (29-35)$$

This equation expresses that the determinant of the system of five linear algebraic equations (29-34) must vanish.

Being a quadratic equation in λ it always has two roots,

$$\lambda = -\frac{1}{2} \left[(\nu + \kappa) \mathbf{k}^2 \pm \sqrt{(\nu - \kappa)^2 (\mathbf{k}^2)^2 + 4\alpha G g_0 \left(1 - \frac{k_z^2}{\mathbf{k}^2}\right)} \right]. \quad (29-36)$$

Both roots are real and one of the roots is evidently negative whereas the other may be positive. The condition that the second root also be negative is,

$$(\nu + \kappa) \mathbf{k}^2 > \sqrt{(\nu - \kappa)^2 (\mathbf{k}^2)^2 + 4\alpha G g_0 \left(1 - \frac{k_z^2}{\mathbf{k}^2}\right)}.$$

Squaring this inequality it becomes,

$$\boxed{\frac{\alpha G g_0}{\kappa \nu} < \frac{(k_x^2 + k_y^2 + k_z^2)^3}{k_x^2 + k_y^2}}. \quad (29-37)$$

The right hand side depends on the geometry of the fluid container and scales like $|\mathbf{k}|^4 \sim d^{-4}$ where d is a typical length scale for the geometry. The inequality may thus be viewed as a condition on the Rayleigh number of the same form as (29-28). If there is no intrinsic length scale, the minimum of the right hand side is zero, and there can be no stability.

Critical fluctuations

When the stability condition (29-37) is fulfilled with a non-vanishing right hand side, all fluctuations are exponentially damped in time, and the fluid will essentially stay at rest. If a fluctuation violates the stability condition it will grow exponentially with time, resulting in more complicated and sometimes turbulent flow. Right at the critical point where the inequality becomes an equality the largest of the two stability exponents (29-36) will vanish, *i.e.* $\lambda = 0$. This indicates that the critical fluctuations are time independent (for a rigorous proof of this assertion see [10]).

At this point it is better to revert to ordinary space where the critical fluctuations must obey the steady-flow versions of the linearized dynamic equations (29-31)-(29-33),

$$-G v_z = \kappa \nabla^2 \Delta T, \quad (29-38a)$$

$$\frac{\nabla \Delta p}{\rho_0} = \nu \nabla^2 \mathbf{v} + \alpha \Delta T g_0 \mathbf{e}_z, \quad (29-38b)$$

$$\nabla \cdot \mathbf{v} = 0. \quad (29-38c)$$

These equations may in fact be combined into a single equation for the temperature excess ΔT . Taking the divergence of the second equation we get,

$$\frac{1}{\rho_0} \nabla^2 \Delta p = \alpha g_0 \nabla_z \Delta T, \quad (29-39)$$

and using this equation and (29-38a), v_z and Δp can be eliminated from the z -component of the second equation, and we obtain,

$$\boxed{(\nabla^2)^3 \Delta T = \frac{\alpha G g_0}{\kappa \nu} (\nabla^2 - \nabla_z^2) \Delta T.} \quad (29-40)$$

This equation is equivalent to the condition of vanishing determinant (29-35) for $\lambda = 0$, and should be solved with the correct boundary conditions for the geometry of the system. Being a kind of eigenvalue equation, each solution determines a value of the coefficient $\alpha G g_0 / \kappa \nu$, and the one that yields the smallest value determines the point where convection first begins.

For a system of characteristic size d , the Rayleigh number is defined as before,

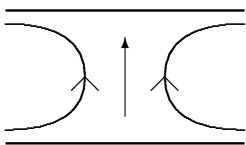
$$\text{Ra} = \frac{\alpha G g_0 d^4}{\kappa \nu}. \quad (29-41)$$

The smallest possible value of this quantity, called the critical Rayleigh number Ra_c , defines the upper limit to convective stability of the baseline state.

The critical fluctuation is apparently another steady solution to the combined heat and mass flow problem. It must however be kept in mind that an essential assumption behind linear stability analysis is that the fluctuation amplitudes are infinitesimal so that non-linear terms can be disregarded. These terms tend in fact to be beneficial and exert a stabilizing influence on the critical field such that it is able to persist somewhat above the critical point. This is in fact why critical fluctuations can be observed at all.

* 29.4 Rayleigh-Bénard convection

Henri Bénard (1874-1939). *French physicist. Discovered hexagonal convection patterns in thin layers of whale oil in 1900. Such cellular convective structures have later been named Bénard cells.*



A rising flow in a horizontal layer of fluid has to veer off horizontally both at the top and the bottom.

Warming a horizontal layer of fluid from below is a common task in the kitchen as well as in industry. It was first investigated experimentally by Bénard in 1900 and later analyzed theoretically by Rayleigh in 1916. The most conspicuous feature of the heated fluid is that convection breaks the original planar symmetry, thereby creating characteristic convection patterns. That the symmetry must break is fairly clear, because it is impossible for all the fluid in the layer to start to rise simultaneously. A localized fluctuation current which begins to rise will have to veer off into the horizontal direction because of the horizontal boundaries. We shall see below that at the onset of convection the flow breaks up into an infinite set of “rollers” with alternating sense of rotation.

Much later in 1956 it was understood that the beautiful hexagonal surface tessellation observed by Bénard in a thin layer of heated whale oil was not caused

by buoyancy alone but was driven by the interplay between buoyancy and temperature dependent surface tension, a phenomenon now called Bénard-Marangoni convection. Here we shall only discuss clean Rayleigh-Bénard convection in layers of fluid so thick that the Marangoni effect can be disregarded.

General solution

Let the horizontal layer of incompressible fluid have thickness d and be subject to a constant negative temperature gradient G . The boundaries are chosen symmetrically at $z = \pm d/2$, for reasons that will be clear in the following. Since the flow has to veer off at the boundaries, the fields must depend on z , implying that $k_z \neq 0$ in the stability condition (29-37). The wave numbers k_x and k_y can in principle take any real values because of the infinitely extended planar symmetry, but since the right hand side of the stability condition diverges for both $k_x^2 + k_y^2 \rightarrow 0$ and $k_x^2 + k_y^2 \rightarrow \infty$, the minimum must occur at a finite value of $k_x^2 + k_y^2$. This argument demonstrates that the critical solution must have a periodic horizontal structure.

For given k_x and k_y we may without loss of generality rotate the coordinate system to obtain $k_y = 0$ and $k_x > 0$, implying that the fields only depend on x and z but not on y . The most general form of the temperature excess then becomes of the form,

$$\Delta T = \Theta \cos k_x x f(z) \quad (29-42)$$

where Θ is a constant, and $f(z)$ is a (so far unknown) dimensionless function of z . From (29-38a) we find the vertical velocity,

$$v_z = -\frac{\kappa\Theta}{G} \cos k_x x (\nabla_z^2 - k_x^2) f(z), \quad (29-43)$$

and from the divergence condition (29-38c) we get the horizontal velocity,

$$v_x = \frac{\kappa\Theta}{Gk_x} \sin k_x x (\nabla_z^2 - k_x^2) f'(z). \quad (29-44)$$

The third velocity component v_y does not participate, but it can be shown (problem 29.3) that it must vanish, $v_y = 0$.

Inserting ΔT into the determinant equation (29-40) we get a sixth order ordinary differential equation for this function,

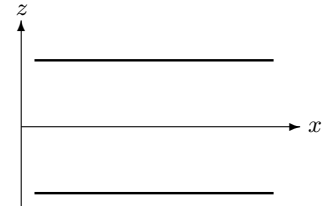
$$(\nabla_z^2 - k_x^2)^3 f(z) = -\frac{\alpha G g_0}{\kappa\nu} k_x^2 f(z). \quad (29-45)$$

Using this relation one may verify that the pressure excess,

$$\frac{\Delta p}{\rho_0} = -\frac{\kappa\nu\Theta}{Gk_x^2} \cos k_x x (\nabla_z^2 - k_x^2)^2 f'(z), \quad (29-46)$$

satisfies (29-39).

Carlo Marangoni (1840-1925). *Italian physicist. Investigated surface tension effects using oil drops spreading on water.*



The plates are placed symmetrically at $z = \pm d/2$.

In a given physical context the actual solution depends on the boundary conditions imposed on the fields. For the temperature excess the boundaries are always assumed to be perfect conductors of heat such that $\Delta T = 0$ for $z = \pm d/2$. For the velocity fields the boundary conditions depend on whether the boundaries are solid plates or free open surfaces. We shall as Rayleigh did in 1916 first analyze the latter case which is by far the simplest.

Two free boundaries

The simplest choice which satisfies the temperature boundary conditions $\Delta T = 0$ for $z = \pm d/2$ is,

$$f(z) = \cos k_z z, \quad k_z = \frac{(1 + 2n)\pi}{d} \quad (29-47)$$

where Θ is an arbitrary (infinitesimal) constant, and $n = 0, 1, 2, \dots$ is an integer. Inserting this into (29-45) and solving for the Rayleigh number we obtain

$$\text{Ra} \equiv \frac{\alpha G g_0 d^4}{\kappa \nu} = \frac{(k_z^2 + k_x^2)^3}{k_x^2} d^4. \quad (29-48)$$

The minimum of the right hand side is found for $k_x = k_z/\sqrt{2}$ and $n = 0$, so that the critical Rayleigh number is,

$$\text{Ra}_c = \frac{27}{4} \pi^4 \approx 657.511 \dots \quad (29-49)$$

The complete critical solution becomes (with $k_x = \pi/d\sqrt{2}$ and $k_z = \pi/d$),

$$\Delta T = \Theta \cos k_x x \cos k_z z, \quad (29-50a)$$

$$v_x = \sqrt{2} U \sin k_x x \sin k_z z, \quad (29-50b)$$

$$v_y = 0, \quad (29-50c)$$

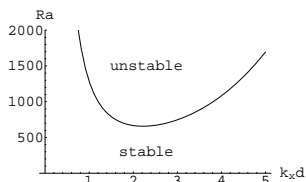
$$v_z = U \cos k_x x \cos k_z z, \quad (29-50d)$$

where $U = 3\pi^2 \kappa \Theta / 2Gd^2$.

The solution is depicted in the three panels of fig. 29.2. The flow pattern (middle panel) consists of an infinite sequence of nearly elliptic “rollers” with aspect ratio $\sqrt{2}$. The temperature pattern (top panel) is 90° out of phase with the flow pattern. This confirms the intuition that the central temperature should be higher when fluid transports heat from the warm lower boundary towards the cold upper boundary, and conversely.

From the above solution we immediately obtain the shear stress,

$$\sigma_{xz} = \eta(\nabla_x v_z + \nabla_z v_x) = \frac{\pi U \eta}{\sqrt{2} d} \sin k_x x \cos k_z z. \quad (29-51)$$



Plot of Ra versus $k_x d$ for $n = 0$. The minimum $\text{Ra} = 27\pi^4/4 \approx 658$ is found at $k_x d = \pi/\sqrt{2} \approx 2.22$

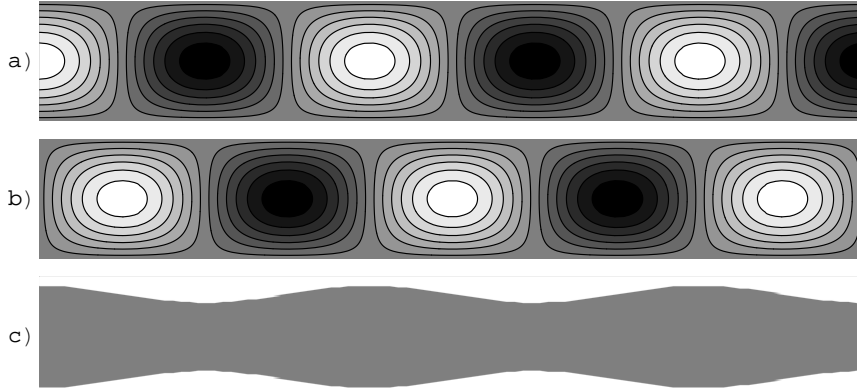


Figure 29.2: *Critical fields in the horizontal layer of fluid with free boundaries (eq. (29-50)). The steady flow pattern consists of an infinity of approximately elliptical rolls of rotating fluid with aspect ratio $\sqrt{2}$ and alternating sense of rotation and temperature excess. a) Contour plot of the temperature field ΔT with high temperature indicated by white. b) Streamlines for the steady flow (v_x, v_z) with white indicating clockwise rotation. c) Deformation of the originally parallel boundaries (strongly exaggerated).*

It evidently vanishes for $z = \pm d/2$, and since we trivially have $\sigma_{yz} = 0$, both boundaries are completely free of shear. There is no practical problem in arranging the upper boundary to be shear-free; that is in fact what we do when we cook. A shear-free lower boundary is on the contrary rather unphysical, so the main virtue of the shear-free model is that it is easy to solve.

The pressure excess in the critical solution may be calculated from (29-46),

$$\Delta p = \frac{2}{3\pi} \alpha \Theta \rho_0 g_0 d \cos k_x x \sin k_z z, \quad (29-52)$$

so that the excess in the normal stress becomes

$$\Delta \sigma_{zz} = -\Delta p + 2\eta \nabla_z v_z = -\frac{10}{9\pi} \alpha \Theta \rho_0 g_0 d \cos k_x x \sin k_z z. \quad (29-53)$$

It does not vanish at the boundaries, showing the solution is not perfect. The non-vanishing normal stress can, however, be compensated by hydrostatic pressure if the layer thickness is allowed to vary a bit. Dividing by $\rho_0 g_0$ we find the required shift at the two boundaries,

$$\Delta z = - \left. \frac{\Delta \sigma_{zz}}{\rho_0 g_0} \right|_{z=\pm d/2} = \pm \frac{10}{9\pi} \alpha \Theta d \cos k_x x. \quad (29-54)$$

The shape of the deformed layer is shown in the bottom panel of fig. 29.2.

Two solid boundaries

A horizontal slot bounded by two solid plates is easy to set up experimentally. Numerous experiments have been carried out in the twentieth century and agree very well with the theoretical results [?].

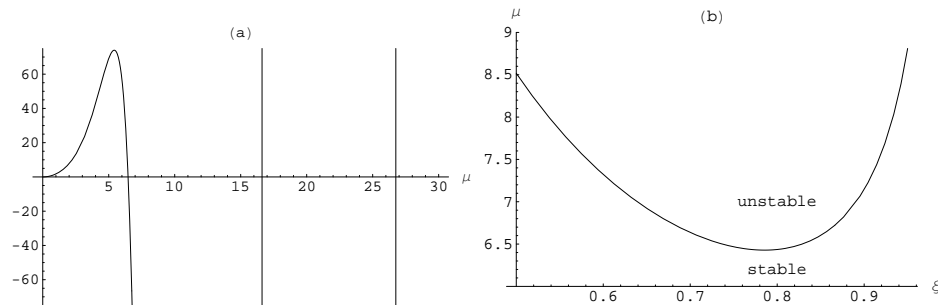


Figure 29.3: *Horizontal slot solution.* **a)** The value of the determinant as a function of μ for $\xi = 0.75$. One notices the regularly spaced solutions where the determinant crosses zero. **b)** Stability plot for the lowest branch as a function of ξ . The minimum $\mu_c = 6.42846 \dots$ for $\xi_c = 0.785559 \dots$ determines the critical Rayleigh number.

For simplicity we choose the plate distance $d = 1$ in the following analysis. The fundamental equation (29-45) is an ordinary 6th order differential equation with constant coefficients, implying that the solution is a superposition of exponentials $e^{\lambda z}$ where λ is a root of the sixth order algebraic equation,

$$(\lambda^2 - k_x^2)^3 = -\text{Ra} k_x^2. \quad (29-55)$$

The six roots are evidently,

$$\lambda = \pm \sqrt{k_x^2 + \text{Ra}^{1/3} k_x^{2/3} \sqrt[3]{-1}}, \quad (29-56)$$

where $\sqrt[3]{-1} = -1, (1 \pm i\sqrt{3})/2$ is any one of the three third roots of -1 . Parameterizing $k_x = \mu\xi^3$ with $\mu = \text{Ra}^{1/4}$, the roots may be written $\lambda = \pm\mu\xi\sqrt{\xi^4 + \sqrt[3]{-1}}$. Assuming $0 < \xi < 1$, the roots take the form $\lambda = \pm i\mu_0$ and $\lambda = \pm\mu_1 \pm i\mu_2$, where

$$\mu_0 = \mu\xi\sqrt{1 - \xi^4}, \quad (29-57a)$$

$$\mu_1 = \frac{1}{2}\mu\xi\sqrt{1 + 2\xi^4 + 2\sqrt{1 + \xi^4 + \xi^8}}, \quad (29-57b)$$

$$\mu_2 = \frac{1}{2}\mu\xi\sqrt{-1 - 2\xi^4 + 2\sqrt{1 + \xi^4 + \xi^8}}. \quad (29-57c)$$

These quantities are all real for $0 < \xi < 1$.

The boundary conditions are in this case $\Delta T = 0$ and $v_x = v_z = 0$ at $z = \pm 1/2$. Since the boundary conditions as well as the fundamental equation (29-45) are invariant under change of sign of z , it follows that the solutions are either symmetric (even) or antisymmetric (odd) in z . In the even case we have,

$$f(z) = A \cos \mu_0 z + B \cosh \mu_1 z \cos \mu_2 z + C \sinh \mu_1 z \sin \mu_2 z, \quad (29-58)$$

where A, B , and C are constants. From the general solution (29-42), (29-43), and (29-44) we see that $f(z)$, $f''(z)$, and $f'''(z) - k_x^2 f'(z)$ must vanish for $z = 1/2$.

The boundary conditions provides three homogenous equations for the determination of A, B , and C . Such equations only have a non-trivial solution if their

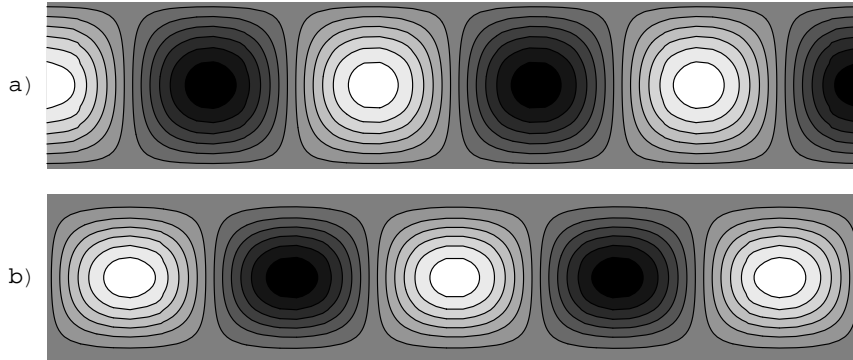


Figure 29.4: *Critical fields in a horizontal layer with solid boundaries. The steady flow pattern consists of an infinity of approximately circular cylindrical rolls of fluid with alternating sense of rotation and alternating temperature excess. a) Contour plot of the temperature field ΔT with high temperature indicated by white. b) Streamlines for the steady flow (v_x, v_z) with white indicating clockwise rotation. Notice how the streamlines “shy away” from the solid walls because of the no-slip conditions.*

3×3 determinant vanishes. It takes a bit of algebra to show that the determinant is proportional to,

$$\det(\mu, \xi) \propto \mu_0 (\cosh \mu_1 + \cos \mu_2) \sin \frac{\mu_0}{2} + ((\mu_1 + \sqrt{3} \mu_2) \sinh \mu_1 + (\mu_2 - \sqrt{3} \mu_1) \sin \mu_2) \cos \frac{\mu_0}{2}. \quad (29-59)$$

Solving the transcendental equation, $\det(\mu, \xi) = 0$, yields a family of solutions $\mu = \mu(\xi)$, as shown in fig. 29.3a. The minimum of the lowest branch determines the critical values $\mu_c = \text{Ra}_c^{1/4} = 6.42846\dots$ and $\xi_c = 0.785559\dots$ (see fig. 29.3b). The critical Rayleigh number becomes (see also problem 29.4 for an approximative calculation)

$$\boxed{\text{Ra}_c = 1707.76\dots} \quad (29-60)$$

and the corresponding wave numbers,

$$\mu_0 = 3.9737\dots \quad \mu_1 = 5.19439\dots \quad \mu_2 = 2.12587\dots \quad (29-61)$$

Finally, solving the boundary conditions at the critical point, the coefficients become (apart from an overall factor),

$$A = 1 \quad B = 0.120754\dots \quad C = 0.00132946\dots \quad (29-62)$$

From these values the actual fields ΔT , v_z , and v_x may be determined. As can be seen from fig. 29.4 the critical flow pattern consists of an infinity of roughly circular cylindrical rolls, which because of the no-slip conditions appear to “shy away” from the boundaries.

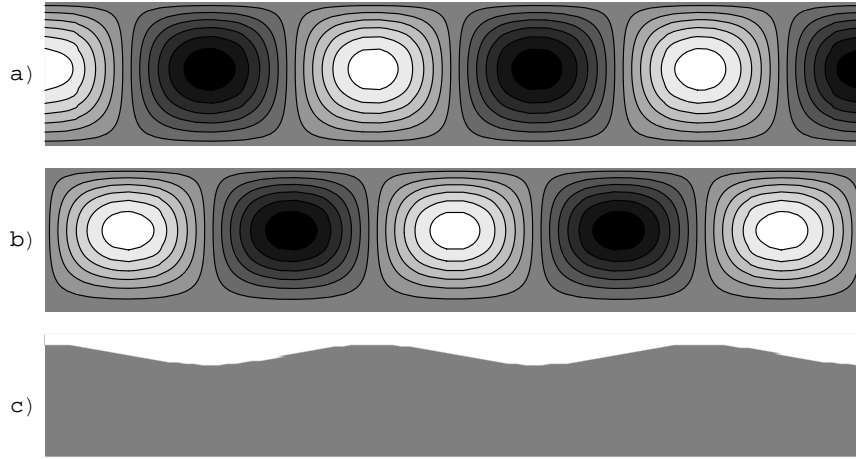


Figure 29.5: *Critical fields in the horizontal layer of fluid with solid bottom and free top. a) Contour plot of the temperature field ΔT with high temperature indicated by white. b) Streamlines for the steady flow with white indicating clockwise rotation. Notice how the no-slip condition makes the streamlines “shy away” from the bottom while it “hugs” the free surface at the top. c) Deformation of the originally flat upper boundary (strongly exaggerated).*

Finally, it should be mentioned that the antisymmetric case,

$$f(z) = D \sin \mu_0 z + E \cosh \mu_1 z \sin \mu_2 z + F \sinh \mu_1 z \cos \mu_2 z , \quad (29-63)$$

is treated in the same way and leads to a critical Rayleigh number of $Ra_c \approx 17610.4 \dots$ which is uninteresting because it is (much) larger than the even solution.

Solid bottom and free top

This is the situation most often found in the household and industry. Since the boundary conditions are asymmetric, the solution is a superposition of all six possibilities,

$$f(z) = A \cos \mu_0 z + B \cosh \mu_1 z \cos \mu_2 z + C \sinh \mu_1 z \sin \mu_2 z \\ + D \sin \mu_0 z + E \cosh \mu_1 z \sin \mu_2 z + F \sinh \mu_1 z \cos \mu_2 z . \quad (29-64)$$

Although more complicated, the solution is found in the same way as before, and the critical values are $\mu_c = 5.75986 \dots$ and $\xi_c = 0.775115 \dots$, and thus the Rayleigh number,

$$\boxed{Ra = 1100.65 \dots} \quad (29-65)$$

This value is probably by accident nearly the same value as the estimate for a rising bubble (29-28). The wave numbers for this solution are

$$\mu_0 = 3.56895 \dots , \quad \mu_1 = 4.55531 \dots , \quad \mu_2 = 1.8947 \dots , \quad (29-66)$$

and the coefficients,

$$\begin{aligned} A &= 1, & B &= 0.086726\dots, & C &= -0.00956513\dots, \\ D &= 0.216993\dots, & E &= 0.00778275\dots, & F &= -0.08632\dots, \end{aligned} \quad (29-67)$$

again apart from an overall factor.

Energy balance?

Where does the energy to drive the rolls come from? The steadily rotating fluid could in principle be set to do useful work, and according to the First Law of thermodynamics this work must be taken from the heat flowing between the plates. In effect the plates act as heat reservoirs and the convection as a heat engine converting heat to work by means of the buoyancy of warm fluid. In the present setup all the work done by the rotating fluid is actually dissipated back into heat by internal viscous forces, so in the steady state the energy of the fluid is constant, and no steady inflow of heat into the system is required. The local heat flow through the boundaries will, however, be uneven because of the local variations in the temperature gradient.

Convective pattern formation

The spontaneous formation of convection patterns in otherwise featureless geometries is a common occurrence. The non-linear terms which have been left out in the linear approximation will exert a stabilizing influence on the patterns such that they are able to persist at Rayleigh numbers somewhat larger than the critical one. At still larger Rayleigh numbers, the rolls of the critical pattern will develop further instabilities and eventually turbulent convection may result (for an account of convection patterns with numerous photographs see [65]).

Problems

29.1 Calculate the critical Rayleigh number for a vertical “chimney” with perfectly conducting walls and a quadratic cross section of size $d \times d$ (it may be assumed that $v_x = v_y = 0$).

29.2 Find an approximative expression for the roots of $\cos x \cosh x = 1$. Calculate the first positive root and its numerical error.

29.3 Show that $v_y = 0$ in the Rayleigh-Bénard solution.

29.4 Show that an approximate solution to the vanishing determinant (29-59) for Rayleigh-Bénard flow in a horizontal slot is

$$\mu = 2 \frac{\mu}{\mu_0} \left(\pi - \arctan \frac{\mu_1 + \sqrt{3}\mu_2}{\mu_0} \right) \quad (29-68)$$

where the right hand side only depends on ξ . Show that the minimum of this function occurs at $\mu = 6.44397\dots$ and $\xi = 0.787942\dots$, corresponding to a critical Rayleigh number $\text{Ra}_c = 1724$.

29.5 Show that the total internal energy is conserved for planar heat diffusion (28-16).

29.6 Show that the spherical temperature distribution

$$T(r) = T_0 + \Theta \left(\frac{a^2}{a^2 + 4\kappa t} \right)^{3/2} \exp \left(-\frac{r^2}{a^2 + 4\kappa t} \right) \quad (29-69)$$

is a solution to Fourier’s equation (28-14).

29.7 Consider two plates at $y = y_1$ and $y = y_2$ and fixed temperatures T_1 and T_2 . Show that if there is incompressible fluid at rest between the plates, the temperature in the fluid is,

$$T = T_1 + (T_2 - T_1) \frac{y - y_1}{y_2 - y_1}. \quad (29-70)$$

Show that this is also true if the fluid is inviscid and moves steadily along x .

29.8 Consider two coaxial cylinders with radii a_1 and a_2 and incompressible fluid at rest between. Show that the temperature distribution between the cylinders is

$$T = T_1 + (T_2 - T_1) \frac{\log(r/a_1)}{\log(a_2/a_1)} \quad (29-71)$$

Show that this is also true if the fluid is inviscid and moves steadily along z .

29.9 Show that there cannot be hydrostatic equilibrium in vertical gravity with horizontal temperature differences. Estimate the speed with which the fluid rises.

29.10 Calculate the ratio between the exit heat flow \dot{Q} and the heat flow \dot{Q}_0 out of the warm plate in a vertical slot as a function of the plate dimensions. Show that this ratio (called the Nusselt number) is

$$\text{Nu} = \frac{\dot{Q}}{\dot{Q}_0} = \frac{1}{45} \cdot \frac{d}{h} \cdot \text{Ra} \quad (29-72)$$

where Ra is the Rayleigh number.

